Journal of Chemistry and Technologies
pISSN 2663-2934 (Print), ISSN 2663-2942 (Online).
journal homepage: http://chemistry.dnu.dp.ua

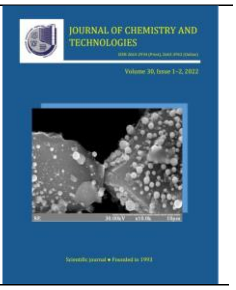
JOURNAL OF CHEMISTRY AND TECHNOLOGIES
Volume 30, Issue 1-2, 2022

UDC 544.65

KINETICS AND MECHANISM OF ELECTROCHEMICAL OXYGEN EVOLUTION IN AN ALKALINE SOLUTION ON NICKEL COATINGS

Vyacheslav S. Protsenko*, Tetyana E. Butyrina, Felix I. Danilov
Ukrainian State University of Chemical Technology, 8 Gagarin Ave., Dnipro, 49005, Ukraine
Received 29 November 2021; accepted 7 February 2022; available online 27 April 2022

Abstract

This work reports about the kinetics and mechanism of the anodic oxygen evolution reaction occurring in an aqueous alkaline solution on two types of nickel electrodes obtained by electrodeposition technique. The first type of nickel coating was deposited from «ordinary» aqueous chloride nickel plating bath. The second type of nickel coating was deposited from an electrolyte based on ethaline (a eutectic mixture of choline chloride and ethylene glycol), which is a typical representative of the so-called deep eutectic solvents (a new generation of room-temperature ionic liquids). The electrocatalytic activity of Ni coatings towards the oxygen evolution reaction was evaluated by linear voltammetry and electrochemical impedance spectroscopy. Under conditions of moderate polarization, the rate-determining step at both types of electrodes is the transfer of the second electron. As the polarization increases, the transfer of the first electron becomes the rate-controlling step. Ni coating electrodeposited from an ethaline-based electrolyte exhibits higher electrocatalytic activity than the coating obtained from an aqueous electrolyte, which is confirmed by higher exchange current densities and lower polarization resistances. The observed effects are due to the manifestation of "true" electrocatalytic activity, rather than a consequence of an increase in the surface area available for the electrochemical process.

Keywords: oxygen evolution reaction; kinetics; mechanism; electrocatalysis; nickel; electrodeposition; deep eutectic solvent.

КІНЕТИКА І МЕХАНІЗМ ЕЛЕКТРОХІМІЧНОГО ВИДІЛЕННЯ КИСНЮ У ЛУЖНОМУ РОЗЧИНІ НА НІКЕЛЕВИХ ПОКРИТТЯХ

Вячеслав С. Проценко*, Тетяна Є. Бутиріна, Фелікс Й. Данилов
ДВНЗ "Український державний хіміко-технологічний університет", просп. Гагаріна, 8, м. Дніпро, 49005, Україна

Анотація

Вивчені кінетичні закономірності і охарактеризований механізм анодного виділення кисню з водного лужного розчину на двох типах нікелевих електродів, одержаних методом електроосадження. Перший тип нікелевого покриття був отриманий зі «звичайного» водного хлоридного електроліту нікелювання. Другий тип нікелевого покриття був осаджений з електроліту на основі ethaline (евтектична суміш холін хлориду і етиленгліколю), що є типовим представником так званих низькотемпературних евтектичних розчинників (нового покоління низькотемпературних іонних рідин). Електрокаталітичні характеристики Ni покриттів у реакції виділення кисню оцінювали методами лінійної вольтамперометрії і спектроскопії електродного імпедансу. За умов помірної поляризації лімітувальною стадією на обох типах електродів є перенесення другого електрона. При зростанні поляризації уповільненим стає перенесення першого електрону. Ni покриття, електроосаджене з електроліту на основі ethaline, демонструє більш високу електрокаталітичну активність, ніж покриття, отримане з водного електроліту, що підтверджується більшими густинами струму обміну і меншими поляризаційними опорами. Спостережені ефекти є наслідком не стільки зростання площі поверхні, доступної для електрохімічного процесу, скільки проявом "істинної" електрокаталітичної активності.

Ключові слова: реакція виділення кисню; кінетика; механізм; електрокаталіз; нікель; електроосадження; низькотемпературний евтектичний розчинник.

**Corresponding author: e-mail: vprotsenko7@gmail.com*

doi: 10.15421/jchemtech.v30i1.245490

Introduction

The development of new, highly efficient and inexpensive electrocatalysts for the process of water electrolysis is an important task of modern electrochemical science in the framework of creating environmentally friendly hydrogen energy [1–3]. In this context, the improvement of electrocatalytic materials for the anodic oxygen evolution reaction is one of the key tasks [2–8]. A relatively high energy barrier of the electrochemical oxygen evolution reaction is the cause of this process significant electrode polarization, which leads to an extremely undesirable increase in voltage on the cell and a corresponding increase in energy consumption. Many attempts have been made to improve the electrocatalytic characteristics of electrode materials in relation to the oxygen evolution reaction by selecting new electrode materials and modifying existing ones. In particular, electrocatalysts based on precious metal oxides (ruthenium and iridium) are widely used [4], the obvious disadvantages of which are high cost and scarcity. It is advisable to develop anode materials based on cheaper base metals, among which much attention is drawn to nickel and its oxides [9; 10]. The advantages of nickel include not only relatively high catalytic activity and availability, but also its bifunctionality (i.e. the ability to use for both anodic oxygen evolution and cathodic hydrogen evolution). In addition, nickel-based electrocatalysts can be easily and controllably produced by electroplating technique. In particular, the possibility of electrochemical deposition of electrocatalytic Ni coatings from electrolytes based on a new class of ionic liquids, the so-called deep eutectic solvents (DESs) has recently been shown [11–13]. It should be observed that DESs are an available, relatively cheap and environmentally friendly alternative to traditional room-temperature ionic liquids, and the use of DESs in electrochemical processes, including electrodeposition, has been the subject of a number of publications over the past two decades [14–17].

The electrocatalytic behavior of nanocrystalline nickel coatings deposited from electrolytes based on DESs with respect to the reaction of cathodic hydrogen evolution was considered in detail earlier [11; 18]. As for the use of Ni electrodeposits fabricated in DES-based electrolytes as electrocatalysts for the oxygen evolution reaction, only an increase in activity was observed as compared to the coating obtained from a "common" aqueous nickel electrolyte [19]. However, the kinetics and possible mechanism of electrocatalytic action of this type of electrodeposited nickel electrocatalysts were not elucidated. This work is devoted to clarifying this issue.

Experimental and Methods

To prepare nickel plating electrolyte, the so-called ethaline was used, this DES being a mixture of ethylene glycol and choline chloride in a eutectic molar ratio (2:1, respectively) [17]. A detailed description of the preparation of electrolyte based on ethaline, containing 1 M $NiCl_2 \cdot 6H_2O$, is given elsewhere [11; 19; 20]. For comparison, nickel coatings were also deposited from an aqueous chloride electrolyte containing 1 M $NiCl_2 \cdot 6H_2O$, 0.5 M NaCl and 0.2 M H_3BO_3 (pH 4).

The coatings were deposited on a Cu substrate made of copper foil, which was thoroughly degreased and activated in hydrochloric acid solution for several minutes. The visible surface area of the electrodes was 1 cm^2. Nickel anodes (without separation of electrode spaces) were used in all electrodeposition experiments. The deposition was performed at the temperature of 40 °C and the current density of 10 mA cm^{-2}. The electrolysis duration was adjusted so that the thickness of the fabricated coatings was about 10 μm. After electrodeposition, the samples were thoroughly washed with double-distilled water and air-dried.

The electrocatalytic behavior of the deposited Ni coatings with respect to the anodic oxygen evolution reaction was studied using a deaerated aqueous solution of 1 M NaOH as the electrolyte. The experiments were conducted in a glass thermostated cell (298 K) using freshly as-deposited nickel coatings as a working electrode. A platinum mesh serves as a counter electrode. The potentials were measured relative to the saturated silver chloride reference electrode and recalculated to the scale of a reversible hydrogen electrode. Voltammetric curves and electrochemical impedance spectra were recorded by means of a Reference 3000 potentiostat (Gamry, USA). Determination of the parameters of elements in the adopted equivalent circuit in electrochemical impedance studies was performed using software built into the potentiostat.

Results and Discussion

Preliminary experiments have shown that the anodic currents on the voltammograms of the nickel electrode in 1 M NaOH solution, corresponding to the electrochemical oxygen evolution, are very sensitive to the state of the electrode surface and its preliminary preparation. In other words, the anode currents are very sensitive to the previous history of the electrode. This behavior is obviously due to the complex chemical and electrochemical transformations that occur on the nickel surface under conditions of anodic polarization in an aqueous medium and contact with atmospheric oxygen. According to the literature [21], upon contact with an alkaline medium, the nickel surface is spontaneously covered with a layer of hydroxide α-$Ni(OH)_2$, which as a result of aging can be dehydrated and recrystallized with the formation of β-$Ni(OH)_2$. It is obvious that the anodic polarization leads to additional electrochemical transformations between hydroxide forms, which greatly affects the electrocatalytic behavior of the coating in relation to the reaction of oxygen evolution. In this paper, we did not set ourselves the task of studying the influence of the transformations of various chemical states of nickel hydroxides films on their electrocatalytic behavior. Therefore, to ensure analysis of different types of coatings in comparable conditions, we, in accordance with the previously reported recommendations [21; 22], performed pre-electrochemical treatment of the surface of Ni samples at the potential of 0.9 V relative to the potential of a reversible hydrogen electrode for 5 min. Such pre-treatment of nickel surface provides effective and reproducible reduction of nickel hydroxide compounds [21]. We found that potentiostatic processing at the above-mentioned electrode potential and duration allows obtaining well-reproduced experimental data.

Fig. 1 shows the polarization curves of anode processes on nickel coatings deposited from an aqueous electrolyte and from an ethaline-based electrolyte. It should be stressed that as is traditionally accepted in the studies of anodic oxygen evolution [23], the electrode potentials are here and below given relative to the scale of the reversible hydrogen electrode, which was calculated by the Nernst equation:

$$E_{\mathrm{RHE}} = -0.059\,pH \qquad (1)$$

According to the published data [24], it was assumed that the *pH* value in 1 M NaOH solution is equal to 13.85. Then the equilibrium potential of the oxygen electrode will be equal to 1.229 V in the scale of the reversible hydrogen electrode, regardless of the pH value of an electrolyte.

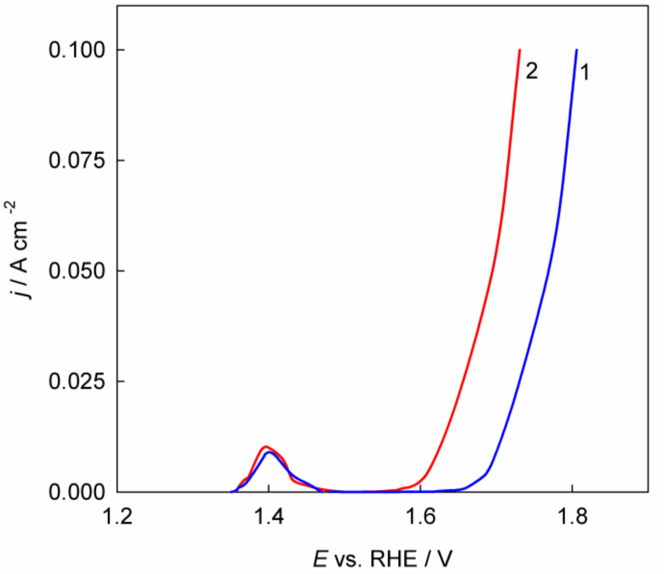

Fig. 1. Anodic polarization curves recorded on Ni coatings deposited from an aqueous chloride electrolyte (1) and from an electrolyte based on ethaline (2) in 1 M NaOH solution at 298 K. Potential scan rate 20 mV s^{-1}

The polarization dependences exhibit a peak of the anode current at the potential of about 1.4 V and exponential regions corresponding to the anodic evolution of oxygen. The current peak at 1.4 V almost coincides in its shape and location for both of the studied electrodes and according to the literature [21] can be ascribed to the anodic oxidation of Ni(II)→Ni(III) in the redox system $Ni(OH)_2/NiOOH$. With regard to the region of oxygen evolution reaction, the obtained data show that the polarization of the process is significantly lower when using a nickel coating from the electrolyte based on DES than when using nickel deposit from «ordinary» aqueous solution, i.e. there is a clear electrocatalytic effect. To obtain appropriate quantitative information about the kinetics of the process of oxygen evolution, the dependences were plotted in the coordinates of the Tafel equation:

$$\eta = a + b \lg j, \qquad (2)$$

where η is the polarization of the electrochemical reaction of oxygen evolution; *a* and *b* are the respective Tafel constants; and *j* is the current density (A cm^{-2}).

It should be noted that the polarization was calculated based on the data on the electrode potential (Fig. 1) according to the equation:

$$\eta = E - 1.229. \qquad (3)$$

It is seen that two linear regions are observed on the graphs plotted in the coordinates of the Tafel equation (Fig. 2): section **I** at relatively low (moderate) polarizations and section **II** at higher polarizations. The corresponding constants of the Tafel equation were determined for both linear sections of the obtained dependences (Table 1). In addition, the values of the exchange current density for oxygen evolution reaction (j_0) were calculated using the following expression:

$$j_0 = 10^{-\frac{a}{b}}. \qquad (4)$$

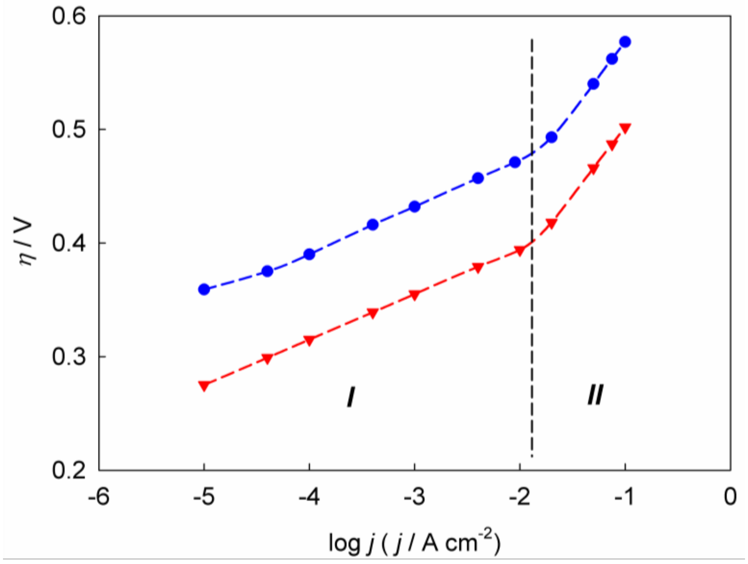

Fig. 2. Tafel dependences for the process of oxygen evolution on Ni coatings deposited from an aqueous chloride electrolyte (1) and from an electrolyte based on ethaline (2) in 1 M NaOH solution at 298 K

Table 1

Kinetic parameters of the reaction of oxygen evolution on Ni coatings in 1 M NaOH calculated from Tafel dependences

Kinetic parameters	Values			
	section I		section II	
	coating from aqueous electrolyte	coating from DES-based electrolyte	coating from aqueous electrolyte	coating from DES-based electrolyte
a / V	0.555	0.475	0.697	0.622
b / V dec^{-1}	0.041	0.040	0.120	0.120
j$_0$ / A cm^{-2}	$2.91 \cdot 10^{-14}$	$1.33 \cdot 10^{-12}$	$1.56 \cdot 10^{-6}$	$6.56 \cdot 10^{-6}$

The most characteristic feature of the obtained data is the appearance of a break on the Tafel dependences, i.e. the formation of two sections with different slopes: the first section at moderate polarizations has a slope of about 40 mV dec^{-1}, and the second section at higher polarizations has a slope of about 120 mV dec^{-1}. Such dependences for the oxygen evolution reaction in alkaline media on nickel electrodes have been repeatedly described in the literature [21; 22; 25]. This behavior is obviously a consequence of the change in the rate-determining step with increasing anodic polarization. Many different reaction mechanisms of this complex reaction have been proposed, and almost all of them involve reactions with the participation of surface oxide, hydroxide and peroxide compounds of nickel in different oxidation states as electrocatalysts [10; 21; 22; 25].

In this work, we used the reaction mechanism developed by Lyons and Brandon [21] to interpret the obtained data. According to this mechanism, the studied process occurs as the following sequence of elementary steps:

$$\left[Ni(III)(OH)_mO_n\right]^{z-} + OH^- \rightarrow \left[Ni(IV)(OH)_{m+1}O_n\right]^{z-} + e^- \qquad (5)$$

$$\left[Ni(IV)(OH)_{m+1}O_n\right]^{z-} \rightarrow \left[Ni(IV)(OH)_{m+1}O_n\right]^{(z-1)-} + e^-, \qquad (6)$$

$$\left[Ni(IV)(OH)_{m+1}O_n\right]^{(z-1)-} + 2OH^- \rightarrow \left[Ni(III)(OH)_{m-1}O_n\right]^{(z-1)-} + 2H_2O + O_2 + e^- \qquad (7)$$

$$\left[Ni(III)(OH)_{m-1}O_n\right]^{(z-1)-} + OH^- \rightarrow \left[Ni(III)(OH)_mO_n\right]^{z-} + e^- \qquad (8)$$

The proposed mechanism (5) – (8) implies that the anionic complex $\left[Ni(III)(OH)_mO_n\right]^{z-}$ (where $z = 2n + m - 3$) acts as an electrocatalyst in the course of oxygen evolution on nickel.

The rates of the first step (5) for the forward and reverse directions of the reaction can be expressed by the following equations (in units of substance flow) [21]:

$$f_1 = k_1^{'0} a_{OH^-}(1-\theta)\exp\left[\frac{\beta F\eta}{RT}\right], \qquad (9)$$

$$f_{-1} = k_{-1}^{'0}\theta\exp\left[-\frac{(1-\beta)F\eta}{RT}\right], \qquad (10)$$

where θ is the degree of electrode surface coverage by adsorbed $\left[Ni(IV)(OH)_{m+1}O_n\right]^{z-}$ particles; $k_1^{'0}$ and $k_{-1}^{'0}$ are the standard electrochemical rate constants; and β is the true transfer coefficient (a symmetry factor).

If the step (5) is in equilibrium, then that allows expressing the value of θ as follows:

$$\theta = \frac{Ka_{OH^-}\exp\left[\frac{F\eta}{RT}\right]}{1 + Ka_{OH^-}\exp\left[\frac{F\eta}{RT}\right]}, \qquad (11)$$

where $K = k_1^{'0}/k_{-1}^{'0}\,k_{-1}^{'0} = \exp\left[-\Delta G^{'0}/RT\right]$.

It is possible to neglect the second term in the denominator of expression (11) at not very high polarizations. Then we get:

$$\theta \cong Ka_{OH^-}\exp\left[\frac{F\eta}{RT}\right]. \qquad (12)$$

The kinetic model developed in work [21] assumes that the transfer of the second electron (Eq. (6)) is the rate-determining step in the chain of transformations (5) – (8) at not very high anode polarization. In this case, the equation for the reaction rate can be written as follows:

$$f_2 = k_2^{'0}\theta\exp\left[\frac{\beta F\eta}{RT}\right]. \qquad (13)$$

Substituting the expression for the value of θ from (12) into formula (13), we finally obtain the equation for the rate of the step (6):

$$f_2 = Kk_2^{'0} a_{OH^-}\exp\left[\frac{(1+\beta)F\eta}{RT}\right]. \qquad (14)$$

The rate of the whole reaction will be determined by the rate of this rate-controlling step. Therefore, it is possible to write the final expression for the rate of oxygen evolution reaction in units of current density:

$$j = 2Ff_2 = 2FKk_2^{'0} a_{OH^-}\exp\left[\frac{(1+\beta)F\eta}{RT}\right]. \qquad (15)$$

If we now assume that the energy barrier during the transfer of the second electron is symmetric (β = 0.5), then the Tafel slope must have the following value:

$$b = \left(\frac{\partial\eta}{\partial \lg j}\right)_{a_{OH^-}} = 2.303\left(\frac{2RT}{3F}\right). \qquad (16)$$

At T = 298 K, we have $b = 0.04$ V dec^{-1}, which coincides well with the experimental data (Table 1).

The nature of the rate-determining step changes in the region of high anodic polarizations and the rate of the whole process begins to be determined by the rate of transfer of the first electron (reaction (5)). In this case, this step ceases to be in equilibrium and its rate is determined by formula (9). Then, we can easily obtain the following expression for the current density of the electrode process:

$$j = 2Ff_1 = 2F = k_1^{'0} a_{OH^-}(1-\theta)\exp\left[\frac{\beta F\eta}{RT}\right]\cdot \qquad (17)$$

As follows from Eq. (17), the Tafel slope in the region of high polarizations will be equal to:

$$b = \left(\frac{\partial\eta}{\partial \lg j}\right)_{a_{OH^-}} = 2.303\left(\frac{2RT}{F}\right). \qquad (18)$$

It is clear that Equation (18) at β = 0.5 and T = 298 K leads to the value of $b = 0.120$ V dec^{-1}, which is observed in the experiment (Table 1).

Analysis of the data given in Table 1 shows that in both regions of the anode polarization curves, the exchange current density for the nickel coating deposited from an ethaline-based electrolyte is significantly higher than that for the nickel coating deposited from an aqueous nickel plating electrolyte. This clearly indicates an increase in electrocatalytic activity. However, this increase in the exchange current density can be caused both by an increase in the surface area available to the electrochemical reaction and by a «true» catalytic effect (i.e. an increase in activity at the same real surface area). Obviously, formal analysis performed using the above kinetic model does not allow discriminating between these effects.

Therefore, the method of measuring the electrochemical impedance was used for a more detailed elucidation of the causes of the observed phenomena. Electrochemical impedance spectra were registered at the electrode potential of 1.6 V relative to the reversible hydrogen electrode, which corresponds to the region of moderate anode polarizations (region **I** for both types of electrodes studied, η = 0.371 V). To interpret the obtained Nyquist diagrams (Fig. 3), we used the known Armstrong-Henderson equivalent circuit [26] (Fig. 4), which has been previously suggested to describe the results of measuring the electrochemical impedance of the oxygen evolution on a nickel oxidized electrode [21].

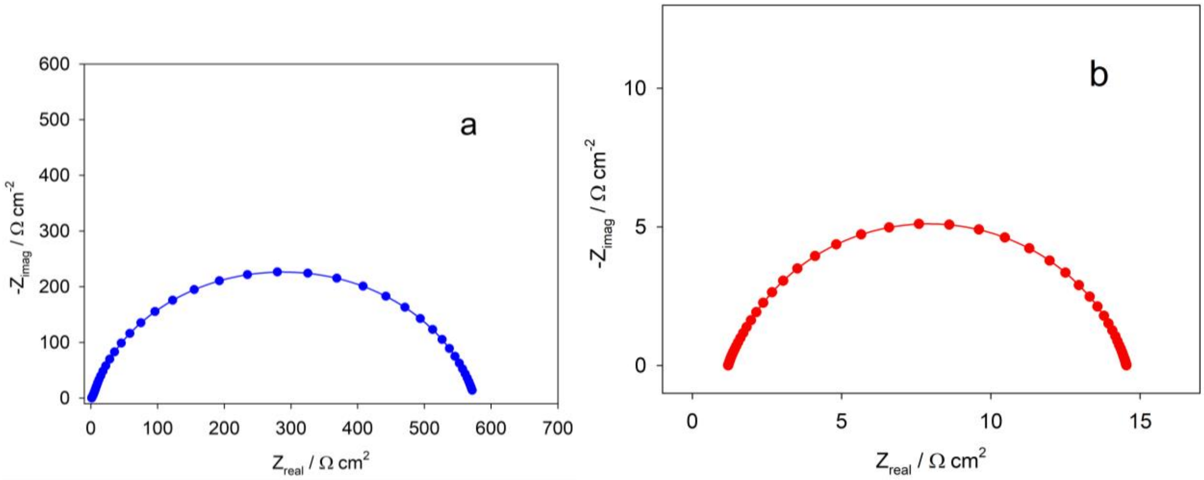

Fig. 3. Nyquist plots obtained by electrochemical impedance spectroscopy on Ni coatings deposited from an aqueous chloride electrolyte (a) and from an electrolyte based on ethaline (b) in 1 M NaOH solution at 298 K

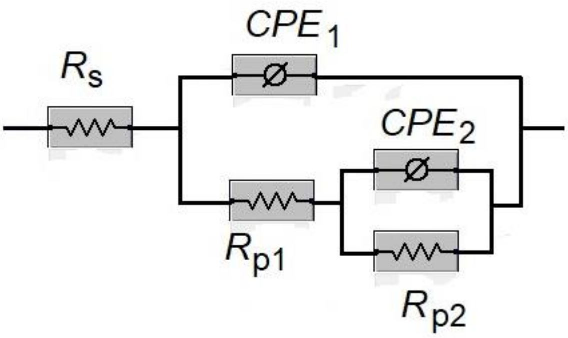

Fig. 4. Equivalent circuit used to simulate the data of electrochemical impedance spectroscopy

The adopted equivalent circuit includes the ohmic resistance of the solution (R_S), the polarization resistances (R_{P1} and R_{P2}) corresponding to two separate successive steps of charge transfer of the electrochemical reaction, and the capacitive impedance components (constant phase elements, CPE_1 and CPE_2) originated from the double electric capacity and pseudocapacity due to adsorption of intermediates, respectively. The calculated parameters of all elements of the equivalent circuit are given in Table 2. It should be mentioned that each constant phase element is characterized by two quantitative parameters: the capacitive component *Q*, which is largely determined by the true surface area available to the electrochemical reaction, and the dimensionless quantity *n*, which reflects phase deviations of the capacitive response of an electrochemical system.

Table 2

Calculated parameters of the elements of equivalent circuit derived from the results of measuring electrochemical impedance of oxygen evolution reaction on nickel coatings in 1 M NaOH at the potential of 1.6 V

Electrode type	R_S / Ω cm^2	R_{P1} / Ω cm^2	Q_1 / μΩ^{-1} s^{n1} cm^{-2}	n_1	R_{P2} / Ω cm^2	Q_2 / μΩ^{-1} s^{n1} cm^{-2}	n_2
coating from aqueous electrolyte	1.3	27.11	396.00	0.834	547.05	72.16	0.941
coating from DES-based electrolyte	1.2	6.43	420.15	0.828	6.912	80.97	0.932

The obtained data show that the polarization resistances (both R_{P1} and R_{P2}) for the coating deposited from the electrolyte based on the DES are significantly lower than the corresponding values for the coating deposited from the aqueous nickel electrolyte. This clearly indicates the increased electrocatalytic activity of electrodeposits fabricated from the DES-containing solution and correlates well with the above voltammetric measurements. For example, the value of R_{P2}, which in the first approximation can be identified with the polarization resistance of the rate-determining step (6), differs for the studied coatings by almost two orders of magnitude. At the same time, for the coating obtained in the DES-based electrolyte, a certain increase in the values of the capacitive components of the constant phase ($Q_{1,\ 2}$) is observed, which indicates an increase in the true surface area, but this effect is not so significant (for example, Q_2 increases only by ~10%). Thus, the above data testify that the main factor in the observed increased electrocatalytic activity of Ni coatings prepared in the ethaline-based electrolyte is not so much an increase in the electrode surface area available to the electrode reaction as a manifestation of "true" catalytic properties. Smaller values of $n_{1,\ 2}$ for the process implemented on nickel deposited from DES-based bath, as compared to nickel derived from the aqueous electrolyte, mean an increase in the degree of energy and geometric inhomogeneity of the electrode surface, which should also improve the catalytic properties. Probably, this is facilitated by the nanocrystalline structure of the nickel coating deposited from the DES-containing electrolyte [11; 27], which causes the formation of more active catalytic sites on the anode surface and/or the growth of their surface concentration. It is worth noting that a similar conclusion was previously made for the cathodic reaction of hydrogen evolution, which proceeds via a completely different mechanism and, obviously, at a different state of the electrode surface.

Conclusions

The kinetics of anodic oxygen evolution on both nickel coatings deposited from aqueous chloride electrolyte and ethaline-based electrolyte was characterized by the methods of linear voltammetry and electrochemical impedance spectroscopy. The oxygen evolution reaction proceeds on both electrode materials via the same mechanism, which at not very high anodic polarizations implies a slow stage of transfer of the second electron. A significant increase in the exchange current density of oxygen evolution and a decrease in the polarization resistance of the electrode reaction in the case of using a coating deposited from an electrolyte based on DES are shown, which is a consequence not so much of increasing the true electrode surface area as a manifestation of "true" electrocatalytic properties.

The data obtained in this work can be used for the development of new electrocatalysts for electrochemical water splitting devices.

Acknowledgements

This work was financially supported by the Ministry of Education and Science of Ukraine (project no. 0121U109551).

References

[1] Lukaczynska, M., Cherigui, E. A. M., Ceglia, A., Van Den Bergh, K., De Strycker, J., Terryn, H., Ustarroz, J. (2019). Influence of water content Grigoriev, S. A., Fateev, V. N., Bessarabov, D. G., Millet, P. (2020). Current status, research trends, and challenges in water electrolysis science and technology. *Int. J. Hydrogen Energy*, 45, 26036–26058. https://doi.org/10.1016/j.ijhydene.2020.03.109

[2] Kovac, A., Paranos, M., Marcius, D. (2021). Hydrogen in energy transition: a review. *Int. J. Hydrogen Energy*, 46, 10016–10035. https://doi.org/10.1016/j.ijhydene.2020.11.256

[3] Lin, R. H., Zhao, Y. Y., Wu, B. D. (2020). Toward a hydrogen society: hydrogen and smart grid integration. *Int. J. Hydrogen Energy*, 45, 20164–20175. https://doi.org/10.1016/j.ijhydene.2020.01.047

[4] Suen, N. T., Hung, S. F., Quan, Q., Zhang, N., Xu, Y. J., Chen, H. M. (2017). Electrocatalysis for the oxygen evolution reaction: recent development and future perspectives. *Chem. Soc. Rev.*, 46, 337–365. https://doi.org/10.1039/c6cs00328a

[5] Qu, H. Y., He, X., Wang, Y., Hou, S. (2021). Electrocatalysis for the oxygen evolution reaction in acidic media: progress and challenges. *Appl. Sci.*, 11, 4320. https://doi.org/10.3390/app11104320

[6] Ishaque, M., Shah, A., Iftikhar, F. J., Akbar, M. (2020). Development of transition metal based electrolyzer for efficient oxygen evolution reaction. *J. Renewable Sustainable Energy*, 12, 024102. https://doi.org/10.1063/1.5123234

[7] Yuan, N., Jiang, Q., Li, J., Tang, J. (2020). A review on non-noble metal based electrocatalysis for the oxygen evolution reaction. *Arab. J. Chem.*, 13, 4294–4309. https://doi.org/10.1016/j.arabjc.2019.08.006

[8] Plevova, M., Hnat, J., Bouzek, K. (2021). Electrocatalysts for the oxygen evolution reaction in alkaline and neutral media. A comparative review. *J. Power Sources*, 507, 230072. https://doi.org/10.1016/j.jpowsour.2021.230072

[9] Vij, V., Sultan, S., Harzandi, A. M., Meena, A., Tiwari, J. N., Lee, W. G., Yoon, T., Kim, K. S. (2017). Nickel-based electrocatalysts for energy related applications: oxygen reduction, oxygen evolution, and hydrogen evolution reactions. *ACS Catal.*, 7, 7196–7225. https://doi.org/10.1021/acscatal.7b01800

[10] Juodkazis, K., Juodkazyte, J., Vilkauskaite, R., Jasulaitiene, V. (2008). Nickel surface anodic oxidation and electrocatalysis of oxygen evolution. *J. Solid State Electrochem*., 12, 1469–1479. https://doi.org/10.1007/s10008-007-0484-0

[11] Protsenko, V. S., Bogdanov, D. A., Korniy, S. A., Kityk, A. A., Baskevich, A. S., Danilov, F. I. (2019). Application of a deep eutectic solvent to prepare nanocrystalline Ni and Ni/TiO_2 coatings as electrocatalysts for the hydrogen evolution reaction. *Int. J. Hydrogen Energy*, 44, 24604–24616. https://doi.org/10.1016/j.ijhydene.2019.07.188

[12] Danilov, F. I., Protsenko, V. S., Kityk, A. A., Shaiderov, D. A., Vasil'eva, E. A., Pramod Kumar, U., Joseph Kennady, C. (2017). Electrodeposition of nanocrystalline nickel coatings from a deep eutectic solvent with water addition. *Prot. Met. Phys. Chem. Surf*., 53, 1131–1138. https://doi.org/10.1134/S2070205118010203

[13] Lukaczynska, M., Cherigui, E. A. M., Ceglia, A., Van Den Bergh, K., De Strycker, J., Terryn, H., Ustarroz, J. (2019). Influence of water content and applied potential on the electrodeposition of Ni coatings from deep eutectic solvents. *Electrochim. Acta*, 319, 690–704. https://doi.org/10.1016/j.electacta.2019.06.161

[14] Smith, E. L., Abbott, A. P., Ryder, K. S. (2014). Deep eutectic solvents (DESs) and their applications. *Chem. Rev*., 114, 11060–11082. http://dx.doi.org/10.1021/cr300162p

[15] Tome, L. I. N., Baiao, V., da Silva, W., Brett, C. M. A. (2018). Deep eutectic solvents for the production and application of new materials. *Appl. Mater. Today*, 10, 30–50. https://doi.org/10.1016/j.apmt.2017.11.005

[16] Hansen, B. B., Spittle, S., Chen, B., Poe, D., Zhang, Y., Klein, J. M., Horton, A., Adhikari, L., Zelovich, T., Doherty, B. W., Gurkan, B., Maginn, E. J., Ragauskas, A., Dadmun, M., Zawodzinski, T. A., Baker, G. A., Tuckerman, M. E., Savinell, R. F., Sangoro, J. R. (2021). Deep eutectic solvents: a review of fundamentals and applications. *Chem. Rev*., 121, 1232–1285. https://doi.org/10.1021/acs.chemrev.0c00385

[17] Abbott, A. P., Ryder, K. S., Konig, U. (2008). Electrofinishing of metals using eutectic based ionic liquids. *Trans. Inst. Met. Finish*., 86, 196–204. http://dx.doi.org/10.1179/174591908X327590

[18] Wang, S., Zou, X., Lu, Y., Rao, S., Xie, X., Pang, Z., Lu, X., Xu, Q., Zhou, Z. (2018). Electrodeposition of nano-nickel in deep eutectic solvents for hydrogen evolution reaction in alkaline solution. *Int. J. Hydrogen Energy*, 43, 15673–15686. https://doi.org/10.1016/j.ijhydene.2018.06.188

[19] Protsenko, V. S., Bogdanov, D. A., Kityk, A. A., Korniy, S. A., Danilov, F. I. (2020). Ni–TiO_2 functional composite coatings deposited from an electrolyte based on a choline-containing ionic liquid. *Russ. J. Appl. Chem*., 93, 1525–1532. http://dx.doi.org/10.1134/S1070427220100067

[20] Danilov, F. I., Kityk, A. A., Shaiderov, D. A., Bogdanov, D. A., Korniy, S. A., Protsenko, V. S. (2019). Electrodeposition of Ni–TiO_2 composite coatings using electrolyte based on a deep eutectic solvent. *Surf. Eng. Appl. Electrochem*., 55, 138–149. http://dx.doi.org/10.3103/S106837551902008X

[21] Lyons, M. E. G., Brandon, M. P. (2008). The oxygen evolution reaction on passive oxide covered transition metal electrodes in aqueous alkaline solution. Part 1 – nickel. *Int. J. Electrochem. Sci*., 3, 1386–1424.

[22] Lyons, M. E. G., Brandon, M. P. (2009). The significance of electrochemical impedance spectra recorded during active oxygen evolution for oxide covered Ni, Co and Fe electrodes in alkaline solution. *J. Electroanal. Chem*., 631, 62–70. https://doi.org/10.1016/j.jelechem.2009.03.019

[23] Tahir, M., Pan, L., Idrees, F., Zhang, X., Wang, L., Zou, J. J., Wan, Z. L. (2017). Electrocatalytic oxygen evolution reaction for energy conversion and storage: a comprehensive review. *Nano Energy*, 37, 136–157. https://doi.org/10.1016/j.nanoen.2017.05.022

[24] Hausmann, J. N., Traynor, B., Myers, R. J., Driess, M., Menezes, P. W. (2021). The pH of aqueous NaOH/KOH solutions: a critical and non-trivial parameter for electrocatalysis. *ACS Energy Lett*., 6, 3567–3571. https://doi.org/10.1021/acsenergylett.1c01693

[25] Lyons, M. E. G., Brandon, M. P. (2010). A comparative study of the oxygen evolution reaction on oxidised nickel, cobalt and iron electrodes in base. *J. Electroanal. Chem*., 641, 119–130. https://doi.org/10.1016/j.jelechem.2009.11.024

[26] Armstrong, R. D., Henderson, M. (1972). Impedance plane display of a reaction with an adsorbed intermediate. *J. Electroanal. Chem. Interf. Electrochem*., 39, 81–90. https://doi.org/10.1016/S0022-0728(72)80477-7

[27] Protsenko, V. S. (2021). Electrodeposition of electrocatalytic coatings in systems based on deep eutectic solvents: a review. *Voprosy Khimii i Khimicheskoi Tekhnologii*, (2), 4–22. http://dx.doi.org/10.32434/0321-4095-2021-135-2-4-22